

The Induced Magnetic Field of Sea Waves

FRED WARBURTON AND RICHARD CAMINITI

*U. S. Naval Ordnance Laboratory
White Oak, Silver Spring, Maryland*

Abstract. Electric currents generated by the circular motion of seawater in the earth's magnetic field give rise to small alternating magnetic fields. These minute fields have the frequency of the ocean waves whipped up by winds. For a 100-m wave with 5-m height, a period of 8 seconds, sea state 6, the field varies from about 3γ at the surface of the sea wave to the order of 0.1γ at a depth of 95 m. This is a less rapid decay than the magnetic field has above the surface due to the same induced currents in the seawater. The component of the field in the direction of propagation reverses direction at a depth of approximately 8 m and reaches a negative maximum at about 24 m. The net effect is a rotating magnetic field in a vertical plane having a cyclic varying amplitude and angular velocity, with forward rotation below the reversal level and reverse rotation above that depth. For a more usual wave (36-m length, 4.8 seconds period, and 0.82-m amplitude, a moderately rough wave in the lower edge of state 4) the field varies from about 0.6γ at the surface to 0.1γ at a depth of 22 m. The reversal of the field component in the direction of propagation of the sea wave in this case occurs at about 3 m.

Introduction. Small magnetic fields of electric currents induced by the motion of the wind-driven sea waves in the earth's magnetic field may be described by the usual electromagnetic theory for conducting mediums. Because seawater is a conducting fluid ($\sigma \approx 4$ mhos/m), its motion in the earth's field produces a transverse magnetic force per unit charge which is the induced electric field that causes the electric currents.

The application of the electromagnetic field equations and boundary conditions to these induced electric fields and the electric currents induced in the seawater has been made by *Longuet-Higgins et al.* [1954]. *Crews and Futterman* [1962] have extended the description to include the induced magnetic fields above the water surface accompanying these currents induced in the water. Both considered the path of the water particles to lie in the vertical xz plane containing the direction x of propagation, and noted that the pure rotational motion of the water, designated by $\nabla \times \mathbf{v} = 0$, need not be assumed. In omitting the so-called displacement current, they determined that there is no appreciable induced current in this plane, as can be seen also in a more elementary way by summing the induced electromotance around a closed path in this plane. Such currents only

need be sufficient to provide the shifting surface charges.

The present study deals with magnetic fields below the water surface induced by the motion of the seawater in the earth's magnetic field. The procedure and the approximations made follow in general those of *Crews and Futterman*, including the designation of the approximately trochoidal wave form. Various solutions [*Lamb*, 1945; *Sverdrup et al.*, 1942] describe the water particles of deep water waves as moving approximately in circles which decrease exponentially with depth. Insofar as the motion of the water particles approximates circular trajectories, the description in terms of trochoidal waves appears sufficient for the induced magnetic fields both below and above the water surface. This idealized case provides important information as to the magnitudes and frequencies of the variations in magnetic fields to be expected.

Induced current density. The radius of the circular path of a water particle is expressed as $r = r_0 e^{-ks}$, where r_0 is the half-height of the wave, the decay constant is $k = 2\pi/\lambda$ with λ the wavelength of the ocean wave, and s is the depth below the mean position of the water at the surface. Figure 1 shows a typical trochoidal sea wave and the exponential decrease of the radius

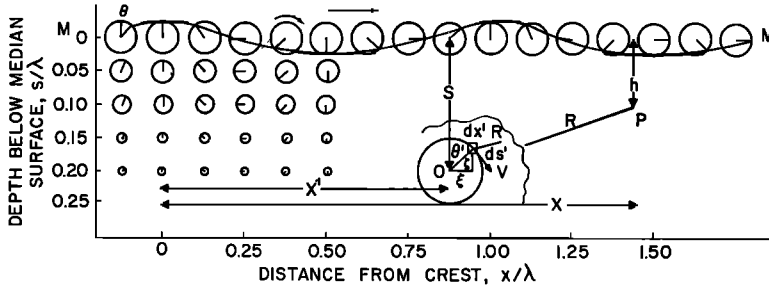


Fig. 1. Diagram of position of water particles at time $t = 0$ in $\cos(\omega t - kx') = \cos \theta'$. The abscissa and ordinate scales indicate the attenuation with depth as a function of wavelength. The abscissa scale is compressed by a factor of 2, and in the insert the source point at O is enlarged to show more detail. The depth s is measured from the mean position MM of the water particles at the surface.

r with depth. The velocity of the water particle has components

$$v_x(x', s, t) = \omega r_0 e^{-ks} \cos \theta' \tag{1}$$

$$v_z(x', s, t) = -\omega r_0 e^{-ks} \sin \theta'$$

where $\theta' = \omega t - kx'$, angular frequency $\omega = 2\pi u/\lambda$, wave velocity $u = (g\lambda/2\pi)^{1/2}$, and x' is the distance of the equilibrium position of the water particle from the yz plane through the origin. If the wave propagation direction x makes a horizontal angle ϵ east of north, and δ is the dip angle, the earth's field has components $B_x = B \cos \delta \cos \epsilon = Bb$, $B_y = B \cos \delta \sin \epsilon$, $B_z = -B \sin \delta = -Ba$. In seawater of conductivity σ , the induced current density should be

$$\mathbf{B}' = \int Idl \times \mathbf{r}/10^7 r^3 = (\mu_0/4\pi) \iiint (\mathbf{J} \times \mathbf{r}) dx' dy' dz'/r^3 \tag{3}$$

for all points Q in the water. The distance r from Q to P (Figure 2) is given by

$$\begin{aligned} r &= \mathbf{i}(x - x' - r_0 e^{-ks} \sin \theta') \\ &\quad + \mathbf{j}(y - y') + \mathbf{k}(s - h - r_0 e^{-ks} \cos \theta') \\ &= \mathbf{i}X_1 + \mathbf{j}Y + \mathbf{k}Z_1 \end{aligned}$$

Using (2) and setting $\mu_0 \sigma u r_0 = 4C$, we can integrate (3) directly with respect to Y from $-\infty$ to $+\infty$. The integration yields, since $dy' = dY$,

$$B_y' = \frac{4BC}{\lambda} \int_0^\infty \int_{-\infty}^\infty \frac{[a \cos(\omega t - kx') - b \sin(\omega t - kx')][s - h - r_0 e^{-ks} \cos(\omega t - kx')]}{[x - x' - r_0 e^{-ks} \sin(\omega t - kx')]^2 + [s - h - r_0 e^{-ks} \cos(\omega t - kx')]^2} e^{-ks} dx' ds \tag{4a}$$

$$B_z' = \frac{4BC}{\lambda} \int_0^\infty \int_{-\infty}^\infty \frac{[a \cos(\omega t - kx') - b \sin(\omega t - kx')][x - x' + r_0 e^{-ks} \sin(\omega t - kx')]}{[x - x' - r_0 e^{-ks} \sin(\omega t - kx')]^2 + [s - h - r_0 e^{-ks} \cos(\omega t - kx')]^2} e^{-ks} dx' ds \tag{4b}$$

$$\begin{aligned} \mathbf{J} &= \mathbf{J}_y = \sigma(\nabla \times \mathbf{B})_y \\ &= \sigma \omega r_0 B e^{-ks} (a \cos \theta' - b \sin \theta') \end{aligned} \tag{2}$$

in any pencil of water of cross section $dx'ds$ and having infinite extent along y .

The induced magnetic field. To find the induced magnetic field \mathbf{B}' at any point $P(xyz)$ (Figure 2) due to elements of current $d\mathbf{J}$ at $Q(x'y'z')$ we integrate the expression for the induced magnetic field

A good approximation for \mathbf{B}' , except at observation points near the surface, is obtained by using the equilibrium points x' and s as the origin of r , as indicated in Figure 2, since the omitted terms ξ and ζ are generally small in comparison with $x - x'$ and $s - h$. This permits integration in closed form, and we substitute $X = x - x'$ for X_1 and $Z = s - h$ for Z_1 for observation points in the water and $Z = s + h$ for points above the water. Hence $dx' = dX$, $ds = dZ$, and $X_1^2 + Z_1^2$ becomes $X^2 + Z^2 = R^2$. If sin

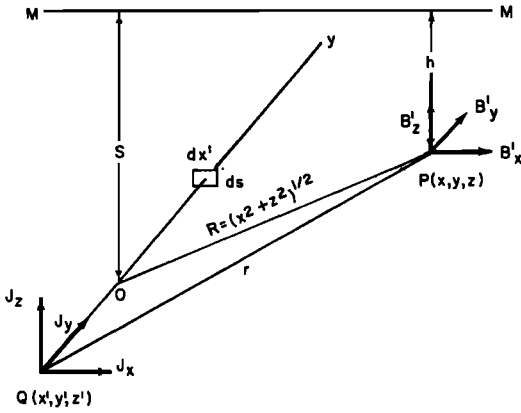


Fig. 2. Magnetic field B' at P due to current elements with components J_x, J_y, J_z at Q . MM represents the mean positions of the surface water particles.

θ' and $\cos \theta'$ are expanded in terms of X and $\theta = \omega t - kx$, the induced magnetic field components become

$$B'_x = \frac{4CB}{\lambda} \int_0^\infty \int_{-\infty}^\infty \frac{e^{-ks}}{X^2 + Z^2} (s \pm h) \cdot [(a \cos \theta - b \sin \theta) \cos kX - (a \sin \theta + b \cos \theta) \sin kX] dX \quad (5)$$

$$B'_z = \frac{4CB}{\lambda} \int_0^\infty \int_{-\infty}^\infty \frac{e^{-ks}}{X^2 + Z^2} \cdot [(a \sin \theta + b \cos \theta) \sin kX - (a \cos \theta - b \sin \theta) \cos kX] X dX$$

The odd functions in X vanish on integration from $-\infty$ to $+\infty$, and the definite integrals,

$$2 \int_0^\infty \frac{\cos kX dX}{X^2 + (s \pm h)^2} = \frac{\pi}{|s \pm h|} e^{-k|s \pm h|}$$

$$2 \int_0^\infty \frac{X \sin kX dX}{X^2 + (s \pm h)^2} = \pi e^{-k|s \pm h|}$$

yield

$$B'_{x\pm} = \frac{4CB}{\lambda} (a \cos \theta - b \sin \theta) \frac{s \pm h}{|s \pm h|} \pi \cdot \int e^{-k|s \pm h|} e^{-ks} ds$$

$$B'_z = \frac{4CB}{\lambda} (a \sin \theta + b \cos \theta) \pi \cdot \int e^{-k|s \pm h|} e^{-ks} ds \quad (6)$$

where the factor $(s \pm h)/|s \pm h| = \pm 1$ has been taken outside the integral sign.

For points P above the water surface, $Z = s + h$ is always positive. Integrating ds from 0 to ∞ yields

$$B'_x = CB(a \cos \theta - b \sin \theta) e^{-2\pi h/\lambda} \quad (7)$$

$$B'_z = CB(a \sin \theta + b \cos \theta) e^{-2\pi h/\lambda}$$

For points P below the water surface, we need to integrate ds from 0 to h for elements of water above the observation point where $s - h \leq 0$ and $|s - h| = h - s$, and integrate ds from h to ∞ for elements of water below the observation point where $s - h \geq 0$ and $|s - h| = s - h$. Then

$$B'_x = CB(a \cos \theta - b \sin \theta) (1 - 4\pi h/\lambda) e^{-2\pi h/\lambda}$$

$$B'_z = CB(a \sin \theta + b \cos \theta) (1 + 4\pi h/\lambda) e^{-2\pi h/\lambda} \quad (8)$$

TABLE 1. Induced Magnetic Field Amplitudes, Sea Wave Moving North*
 $\lambda = 100$ m, $u = 12.5$ m/sec, $r_0 = 2.5$ m, $T = 8$ sec

Depth (Height) $h,$ m	In Water			In Air
	$(B'_x)'_0,$ γ	$(B'_z)'_0,$ γ	$B'_0,$ γ	$(B'_z)'_0 = (B'_x)'_0,$ γ
0	2.200	2.200	3.11	2.200
2	1.492	2.432	2.96	1.942
4	0.850	2.578	2.71	1.712
6	0.370	2.650	2.68	1.510
8	-0.008	2.672	2.67	1.340
10	-0.304	2.663	2.67	1.182
12	-0.527	2.600	2.66	1.036
14	-0.696	2.521	2.62	0.914
16	-0.815	2.425	2.56	0.806
18	-0.900	2.322	2.49	0.711
20	-0.950	2.200	2.40	0.627
23	-0.982	2.023	2.24	0.520
25	-0.980	1.892	2.13	0.458
27	-0.975	1.778	2.02	0.404
30	-0.927	1.593	1.94	0.334
32	-0.892	1.483	1.71	0.295
35	-0.830	1.317	1.56	0.244
40	-0.718	1.075	1.29	0.178
45	-0.608	0.868	1.08	0.131
50	-0.502	0.692	0.86	0.095
55	-0.410	0.546	0.68	0.069
60	-0.332	0.434	0.54	0.051
70	-0.212	0.266	0.34	0.027
80	-0.132	0.161	0.21	0.015
90	-0.079	0.095	0.12	0.008
100	-0.051	0.057	0.08	0.004

* For the purposes of all computations in this report, we take the earth's field to be 0.561 gauss at dip angle 71° , as it is at the Naval Ordnance Laboratory, White Oak, Maryland.

TABLE 2. Induced Magnetic Field Amplitudes, Sea Wave Moving North*
 $\lambda = 36$ m, $r_0 = 0.82$ m, $T = 4.8$ sec, $u = 7.5$ m/sec

Depth (Height) h , m	In Water			In Air
	$(B_x')_0$, γ	$(B_z')_0$, γ	B_0' , γ	$(B_z')_0 = (B_x')_0$, γ
0	0.433	0.433	0.613	0.433
0.5	0.328	0.466	0.566	0.397
1.0	0.234	0.485	0.538	0.360
1.5	0.159	0.502	0.527	0.330
2	0.092	0.518	0.526	0.306
3	-0.012	0.526	0.527	0.257
4	-0.085	0.516	0.523	0.216
5	-0.135	0.497	0.515	0.181
6	-0.167	0.472	0.501	0.152
7	-0.184	0.440	0.477	0.128
8	-0.192	0.407	0.450	0.107
9	-0.193	0.373	0.420	0.090
10	-0.188	0.340	0.388	0.076
12	-0.170	0.277	0.324	0.054
15	-0.134	0.197	0.238	0.032
20	-0.0790	0.1056	0.1319	0.0132
25	-0.0435	0.0548	0.0700	0.0056
30	-0.0218	0.0264	0.0343	0.0023
35	-0.0109	0.0129	0.0169	0.0010
40	-0.0052	0.0060	0.0079	0.0004
45	-0.0025	0.0028	0.0038	0.00017
50	-0.0012	0.0013	0.0018	0.00007

* The statistical relation $\lambda = 44r_0$ [Vine and Volkman, 1950] is used for the $\lambda = 36$ m sea wave.

Tables 1 and 2 show the attenuation, with depth, of the amplitudes $BCe^{-2\pi h/\lambda} (1-4\pi h/\lambda)$ and $BCe^{-2\pi h/\lambda} (1+4\pi h/\lambda)$, for a sea wave moving north, with parameters as indicated in the tables. Also included are the amplitudes for B_x' and B_z' in air.

Figure 3 shows a plot of the data in Tables 1 and 2 of the variations in the amplitude $BCe^{-2\pi h/\lambda} (1-4\pi h/\lambda)$ and $BCe^{-2\pi h/\lambda} (1+4\pi h/\lambda)$ in the x and z components of the induced magnetic field of a northbound plane trochoidal wave, as a function of the dimensionless parameter h/λ . Here, as in Tables 1 and 2, the B_x' and B_z' components of the induced field in the water attenuate much less rapidly with depth than the field at corresponding heights h above the surface. The indicated reversal in direction of x component of the induced field at a depth of approximately 3 meters for the 36-meter wave and 8 meters for the 100-meter wave is due simply to the fact that currents J_y in water above an observation point produce a field opposite in direction to that of currents in water below this point.

For short waves in sea state zero, with $\lambda/r_0 = 14$ and $T = 1$ sec, hence $\lambda = 1.56$ m, $r_0 = 0.112$ m, we deduce that the induced field B' at the surface should be only 0.017γ with B_x' reversing at a depth of 0.12 meter.

Figure 4a presents the values of B_x' , B_z' , and the total induced field B' for the depths $h = 2, 8, 25,$ and 40 m as a function of the horizontal distance x (at $t = 0$ and $\theta = -kx$ in (8)) measured from the peak of the sea wave for $\lambda = 36$ meters moving north at a speed 7.5 m/sec in an earth's field of $B = 0.561$ gauss and 71° dip.

Figure 4b shows the variations of the magnetic field in time at any one place such as $x = 0$. For the wave moving due north B_y' is zero and the field B' appears as a vector, with

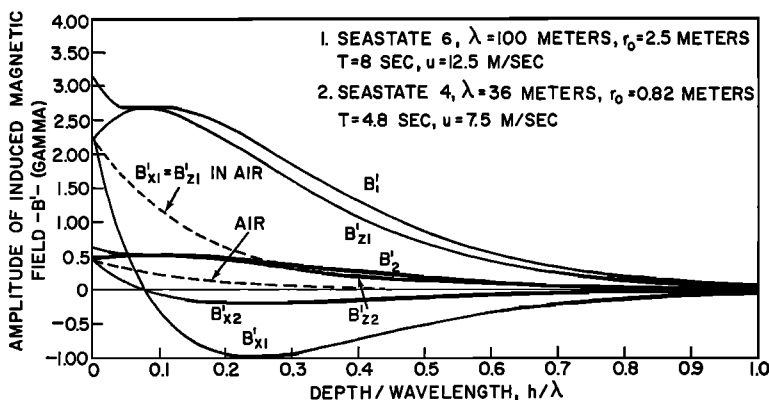


Fig. 3. Magnetic field amplitudes induced by a high sea wave, and by a moderately rough sea wave, north heading.

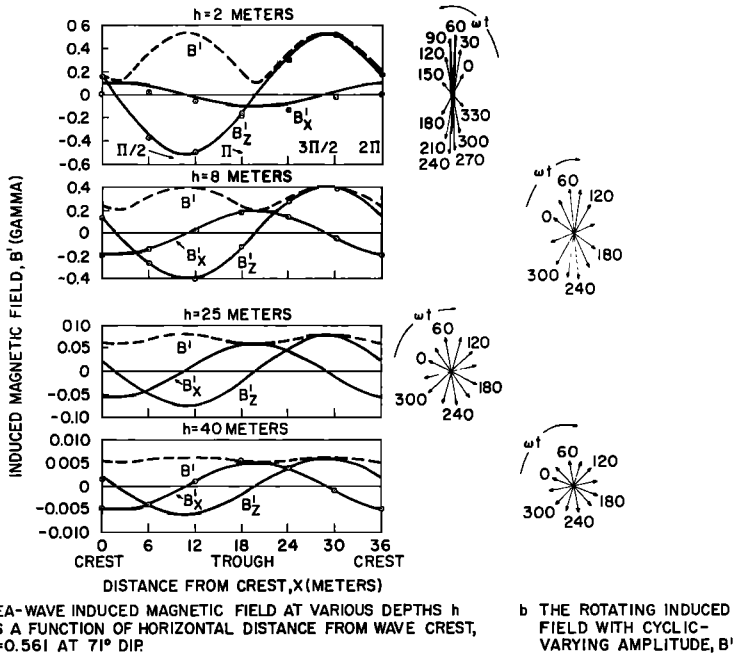


Fig. 4. Pattern of magnetic field induced by the moderately rough sea wave moving north. $\lambda = 36$ m, $r_0 = 0.82$ m, $T = 4.8$ sec., $\omega = 7.5$ m/sec. (a) Diagram at $t = 0$ of the B'_x and B'_z components and their resultant B' . Data points enclosed in circles \odot are obtained by the IBM numerical integration of equations 4a, 4b. (b) Rotation of induced vector field at $x = 0$.

cyclically varying amplitude, rotating in the north-south vertical plane. At depths below the reversal point of B'_z (approximately 3 meters) this is a forward rotation in the direction of the circular motion of the water particles, at points above that level B' has a backward rotation. And this is the same for the wave moving due south.

For a plane trochoidal sea wave traveling due east, the coefficient b in (8) is zero, and the induced magnetic field below the water surface reduces to

$$B'_z = CB(1 - 4\pi h/\lambda)e^{-2\pi h/\lambda} a \cos(\omega t - kx)$$

$$B'_x = CB(1 + 4\pi h/\lambda)e^{-2\pi h/\lambda} a \sin(\omega t - kx) \tag{9}$$

while the field above the water surface (equation 7) reduces to a form like (9), except that the factors $1 - 4\pi h/\lambda$ and $1 + 4\pi h/\lambda$ do not appear. The amplitude of the x and z components of B' differ by the factor a from those for the wave progressing north.

Table 3 presents the values of B'_z and B'_x

and the total induced field B' as a function of h for a sea wave moving east with parameters as indicated.

Figure 5 shows the variations of B'_x and B'_z as a function of sea state, wavelength λ , and height $2r_0$ at various depths $h = 2, 3, 5, 8,$ and 25 m. The statistical relation $\lambda = 44r_0$ is assumed. The solid lines show the variations in the x component of the fields, $B'_x = BCe^{-2\pi h/\lambda}(1 - 4\pi h/\lambda)$, and the dashed lines show the variations in the z component $B'_z = BCe^{-2\pi h/\lambda}(1 + 4\pi h/\lambda)$. Curves for B'_z at $h = 3$ m and 5 m lie between those for $h = 2$ m and 8 m. The points at which the solid lines cross the x axis indicate the wavelength and sea state at which the theory predicts that the x component reverses direction, $\lambda = 100, 63, 38,$ and 25 m at depths $8, 5, 3,$ and 2 m, respectively. The approximate wavelength and sea state at which the x component reaches a negative maximum at each of these depths may also be noted in the neighborhoods of $\lambda = 55, 36, 24,$ and 15 m, respectively. As will be noted below and in Figure 4, the approximation introduced in the theory

TABLE 3. Induced Magnetic Field Amplitudes, Sea Wave Moving East
 $\lambda = 36$ m, $r_0 = 0.82$ m, $T = 4.8$ sec, $u = 7.5$ m/sec

Depth (Height) h , m	In Water			In Air
	$(B_x')_0$, γ	$(B_z')_0$, γ	B_0' , γ	$(B_x')_0 = (B_z')_0$, γ
0	0 409	0 409	0.580	0 409
0.5	0 310	0 440	0.543	0.376
1.0	0 223	0 464	0 514	0 344
1.5	0 151	0 482	0.504	0 314
2.0	0 087	0 490	0 498	0 289
2.86	0	0 496	0.496	0.248
3	-0 011	0 496	0.496	0.242
4	-0.081	0 488	0 495	0.204
5	-0.127	0 470	0.487	0.171
6	-0.158	0 447	0.473	0.144
7	-0.174	0 416	0.450	0.120
8	-0.182	0 385	0.425	0.101
9	-0.182	0 353	0 397	0 0850
10	-0.178	0 322	0 368	0 0715
12	-0.162	0 263	0.308	0.0506
15	-0.126	0 187	0.225	0.0336
20	-0.0746	0.0998	0.125	0.0125
25	-0.0412	0.0518	0.067	0 0052
30	-0 0207	0.0250	0.032	0.0022
35	-0.0103	0 0121	0 016	0 0009
40	-0.0049	0.0057	0.007	0.0004
45	-0.0023	0.0026	0 003	0 0002
50	-0 0014	0 0012	0 002	0 0001

affects the values of B' somewhat only at observation points near the surface.

The error introduced by the approximation that the elements of water in their circular paths of radii $r = r_0 e^{-ks}$ remained at their equilibrium positions but retained their correct velocities was checked by an IBM 7090 computer, which was used to integrate equations 4a and 4b. The integration was performed as follows:

$$B_x' = \frac{4BC\Delta x\Delta s}{\lambda} \sum_{i=1}^n \sum_{j=1}^m \frac{(a \cos kx_i + b \sin kx_i)(s_i - h - r_0 e^{-ks_i} \cos kx_i)e^{-ks_i}}{(x_i - x - r_0 e^{-ks_i} \sin kx_i)^2 + (s_i - h - r_0 e^{-ks_i} \cos kx_i)^2} \quad (10a)$$

$$B_z' = \frac{4BC\Delta x\Delta s}{\lambda} \sum_{i=1}^n \sum_{j=1}^m \frac{(a \cos kx_i + b \sin kx_i)(x_i - x - r_0 e^{-ks_i} \sin kx_i)e^{-ks_i}}{(x_i - x - r_0 e^{-ks_i} \sin kx_i)^2 + (s_i - h - r_0 e^{-ks_i} \cos kx_i)^2} \quad (10b)$$

In making the approximation in the analytic integration, effects of the wave form at the surface are suppressed because the consequence of dropping the terms $r_0 e^{ks} \cos kx'$ and $r_0 e^{-ks} \sin kx'$ not only moves the elements of water from the ends of their radii to their equilibrium position

but also treats the ocean as if it were flat. The IBM 7090 results show that the approximation has little or no effect on either component of the induced field at a depth of 8 m or greater. Nearer the surface, however, the exact solution shows the effect of considering the wave surface in the geometry of the problem.

Figure 4 is a plot of the analytic and numerical integration for the x and z components of field at various depths. At 8 m both solutions produce the same results, but at 2 m the z component differs slightly and the x component is affected rather strongly. An explanation of the asymmetrical behavior of the x component can be gained from an examination of Figure 6, which shows the surface of the ocean and two field points, one at $x = 0$ and the other at $x = 18$ m. These observation points are at a depth of 2 m, as measured from the median level of the ocean, and are surrounded by currents whose directions are indicated by the conventional signs. The sign of the integrand which gives B_x' depends only on the sinusoidal term as x varies and therefore cannot change sign in the vicinity of either of the field points in question. Also, it was found that the series used to compute B_x' converges quite rapidly, which indicates that contributions from distant points are small. Therefore we wish to examine the effect of currents close to the observation points. We see that the distance to the field point at $x = 18$ m from source points around it is of the order of $(h - r_0)$ while the distance from corresponding points at $x = 0$ is $(h + r_0)$. Therefore the field at $x = 18$, from currents which are centered around this point, is stronger than the field of corresponding currents centered around

$x = 0$. It is seen that the major contribution at $x = 18$ is negative and at $x = 0$ it is positive; hence the shapes of the curves.

The z component of the induced field does not vary in a similar manner for two reasons. The integrand for B_z' depends on the difference

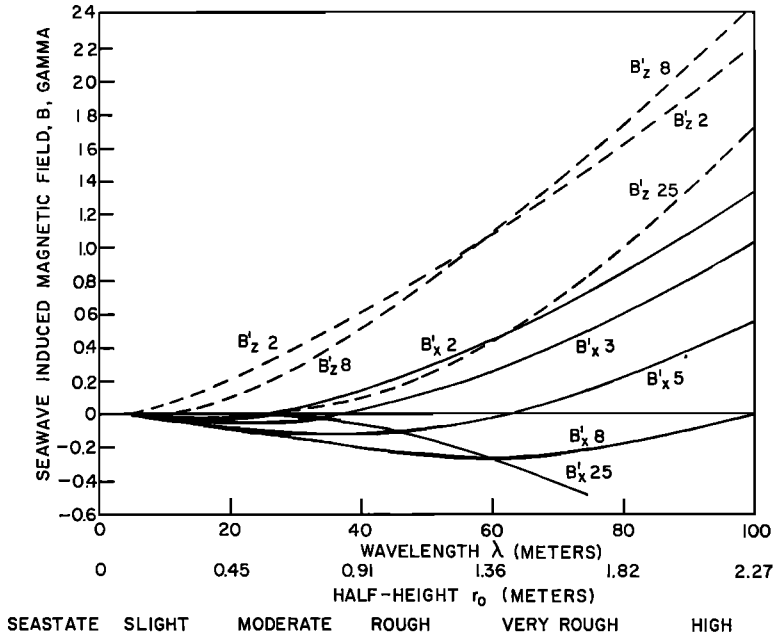


Fig. 5. Variation of induced magnetic field with sea state at depths 2, 3, 5, 8, and 25 m.

($x'-x$), and therefore contributions from currents first to the left of a field point are partly nullified by contributions from currents close by on the right. Also, it was found that the series used to compute B_z' converges quite slowly; therefore, distant source points contribute significantly, and so B_z' escapes the surface effect and closely follows the approximate analytic solution.

Some remarks on the slowly converging series used to compute B_z' should be of interest. The computer was used to determine the field at a depth of 40 m. At this depth, it was expected that the effects of the approximation would vanish and the analytic results would agree with the numerical integration. The x component agreed very well, but the z component differed from the integration in closed form; the amplitude was too small and had the wrong sign. Further investigation showed that the series oscillates as the range of summation in x is changed. Using the analytic expression for B_z' as essentially correct, we found that the numerical integration gave the desired result when the sum over x was carried out to a quarter wavelength, such as 10.25λ instead of 10λ . One calculation which was carried out to 20λ on either

side of the field point showed the numerical integration slowly converging to the analytic integration.

This description of the magnetic field induced by sea waves is developed for waves uniform over a large area. For a localized storm the effect is obviously present but not so well defined. Insofar as the motion of the water particles of a uniform wave is approximated by circular trajectories, the description in terms of tro-

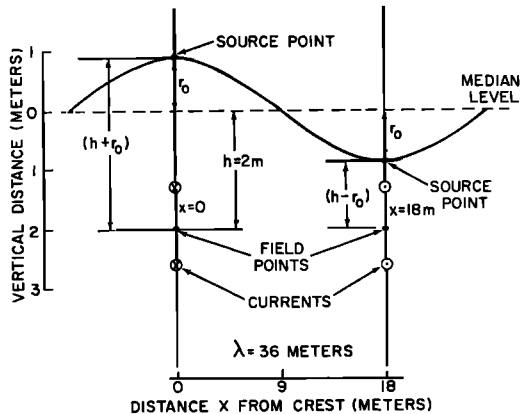


Fig. 6. Field points near the ocean surface.

choidal waves is sufficient for representing the salient features of the induced magnetic fields both below and above the water surface. In any case, this induced magnetic field has the frequency of the water wave, and the magnitude of this field is well within the range of detecting instruments.

Acknowledgment. We wish to express appreciation for the assistance of Mr. Karl Glick in checking the mathematics of this report.

REFERENCES

Crews, A., and J. Futterman, Geomagnetic micropulsations due to the motion of ocean waves, *J. Geophys. Res.*, 67, 299-306, 1962.

Lamb, Horace, *Hydrodynamics*, 6th ed., Dover Publications, p. 368, 1945.

Longuet-Higgins, M. S., M. E. Stern, and H. Stommel, The electrical field induced by ocean currents and waves, with applications to the method of towed electrodes, *Woods Hole Oceanog. Inst., Contrib.* 690, November 1954.

Sverdrup, H. U., M. W. Johnson, and R. H. Fleming, *The Oceans*, 516 pp., Prentice-Hall, 1942.

Vine, A. C., and G. H. Volkman, Wind waves at sea, *Woods Hole Oceanog. Inst. Table*, June 1950.

(Manuscript received March 9, 1964;
revised July 22, 1964.)